Nonlinear Analysis: Modelling and Control, 2003, Vol. 8, No. 1, 19–32

Comparison of 2-D and 3-D Diode-Pumped Solid-State Laser Cooling Models

J. Dabulytė[1], F. Ivanauskas[2]

[1]Vilnius University, Naugarduko 24, 2600 Vilnius, Lithuania
Kaunas Technology University, Studentų 50, 3000 Kaunas, Lithuania
jurgita.dabulyte@ktu.lt

[2]Vilnius University, Naugarduko 24, 2600 Vilnius, Lithuania
Institute of Mathematics and Informatics, Akademijos 24, 2600 Vilnius, Lithuania
feliksas.ivanauskas@maf.vu.lt

Received: 12.03.2003
Accepted: 20.03.2003

Abstract. We propose a cooler of a laser material which compensates the thermal gradients caused by the pump radiation by the gradients created by the cooler. The mathematical model of the system is based on the numerical solution of the heat transfer equation using a finite – difference technique. The 3-D and 2-D computer simulatios were used to investigate the cooling problem and show the reliability of two-dimensional model.

Keywords: diode-pumped solid-state laser, Yb:KGW, laser cooling system, thermal effects.

1 Introduction

High-power, diode-laser-pumped solid-state lasers with excellent beam quality are required in various industrial, military, medical and scientific applications. Due to the specific nature of the some laser materials, high intensity pump beams are required to achieve sufficient inversion in the laser material [1, 2]. However, part of the pump power is transformed into heat in a small volume of the active media. Thermal effects caused by the heat are limiting the efficiency of the laser [3]. The temperature gradient generates:

- Mechanical stresses in the laser material (the hotter inside area is constrained from expansion by the cooler outer zone).

- Photoelastic effects: the stresses generate thermal strains in the laser material, which in turn produce refractive index variation via the photoelastic effect.

- Optical distortion (the change of the refractive index can be separated into a temperature dependant and stress dependant variation).

- Stress birefringence: heat can induce birefringence effect into the material [4].

In order to improve the pumping and generating power of the longitudinal diode-pumped solid-state laser, the issue of an active material cooling should be resolved. The cooling system has an important impact on the laser efficiency. Most of the elements are highly temperature sensible. To minimize the problems that can occur, a reliable and accurate cooling system is required. Naturally, the presence of cooling is essential for the laser diodes but, even more, it is important to control thermal lensing and thermally induced strain in the laser material. There is a lot of possibilities to choose a cooling system [4]:

- Thermo-electric coolers (Peltier devices) can be used. The problem is that they consume twice as much the electrical energy as the heat they remove. Thus, their is prohibitive for high power applications.

- Thermal control systems based on the flow of a coolant liquid are used, too. The laser diodes are mounted on a heat sink with a high thermal conductivity. As the laser efficiency is a function of the temperature of the liquid, refrigerator stages must be inserted into the cooling loop.

- To increase heat dissipation, laser diodes are implemented on a mount with micro-channels. Flowing through these channels, coolant is in contact with a large surface with a very thin boundary layer, thus increasing the heat transfer.

We propose to modify the cooler of the laser material in such a way that thermal gradients caused by the pump radiation would be compensated by the gradients created by the cooler. In mathematical terms, we search for

such boundary conditions, which compensate thermal gradients inside the laser material.

The Yb:KGW crystal was chosen for our experiment. Yb:KGW is one of the most promising laser active materials. A simple two-level electronic structure of the Yb ion avoids undesired loss processes such as upconversion, excited state absorption and concentration quenching. Compared with the commonly used Nd:YAG crystals, the Yb:KGW crystal has a much larger absoption bandwidth, 3 or 4 times longer emission lifetime in similar hosts with enhanced storage capacity, lower quantum defect and is more suitable for diode pumping than the traditional Nd-doped systems. We superimpose over and under the Yb:KGW crystal sapphire slabs and this construction is brazed by the copper. We use sapphire because of its high thermal conductivity. Sapphire is also quite easily processed and does not absorb used wavelength beam. That is very important because the steam should not appear if our shot had missed the crystal during the laser regularizing. If steam appears it can damage the optical surfaces of active element. Therefore, sapphire warrants cleanliness of the optical surfaces.

The laser was end-pumped by laser diode and the output parameters, temperature and temperature gradients were measured. To better understand the system's thermal behavior, we examine the mathematical model. This model is based on the numerical solution of the heat equation with initial and boundary conditions (we use finite-difference technique [5]) .The initial condition express initial temperature in the laser material and the boundary conditions express the flow of heat.

In practice, such problems are solved in 3-D shape. However, in the literature 2-D-in-space laser cooling models have also been used. The advantage of 2-D model is that this model contains less parameters that usualy strongly depend on variables to be found [6]. Also the use of multidimensional models is problematic in practice. The 3-D and 2-D computer simulations were used to show the reliability of two dimensional model.

2 Mathematical Model

We shall transform the laser optimal cooling problem into a simplest physical task to explore the regime of temperature in crystal. The schematic view of the

laser material cooling system is shown in Fig. 1.

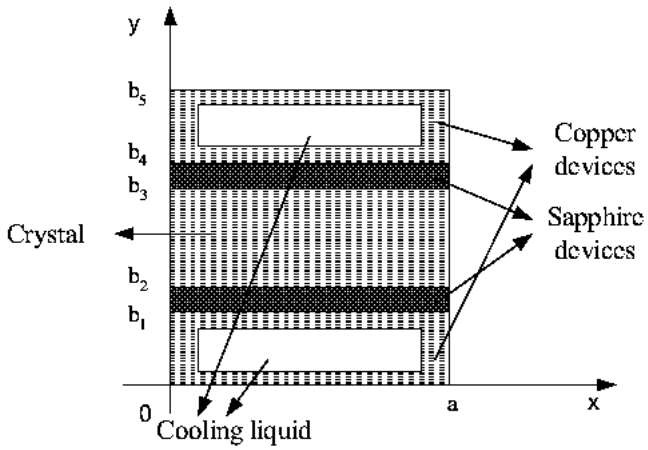

Fig. 1. The schematic view of the laser material cooling task (xy-plane cut).

The pump beam is generated with a high-power diode bar and injected into the $z = 0$ face (also here 2-D and 3-D models would be compared between each other). The Yb:KGW laser crystal is cooled from the top and bottom sides.

Let

a – be the width of crystal, sapphire and cooper devices,

$b' = b_3 - b_2$ – crystal height,

$b'' = b_4 - b_3 = b_2 - b_1$ – sapphire devices height,

$b''' = b_5 - b_4 = b_1$ – copper devices height.

The mathematical model of temperature regime in the laser is based on the heat equation

$$\frac{\partial u}{\partial t} = D_1\Big(\frac{\partial^2 u}{\partial x^2} + \frac{\partial^2 u}{\partial y^2} + \frac{\partial^2 u}{\partial z^2}\Big) + \frac{f(x,y,z)}{Q_1\rho_1}, \qquad (1)$$
$$\Phi = \{0 < x < a,\ b_2 < y < b_3,\ 0 < z < c\},$$

where

$u = u(t,x,y,z)$ – temperature;

t – time;

Q_1 – Yb:KGW crystal specific heat;

ρ_1 – crystal density;

$f(x, y, z)$ – lighting (heating) source;

$D_1 = k_1/Q_1 \cdot \rho_1$ – diffusion coefficient;

k_1 – crystal thermal conductivity.

The temperature regime in the sapphire and in the copper is described by the next differential equations:

in sapphire

$$\begin{aligned} &\frac{\partial u}{\partial t} = D_2\Big(\frac{\partial^2 u}{\partial x^2} + \frac{\partial^2 u}{\partial y^2} + \frac{\partial^2 u}{\partial z^2}\Big), \\ &\Omega_1' = \{0 < x < a,\ b_1 < y < b_2,\ 0 < z < c\}, \\ &\Omega_2' = \{0 < x < a,\ b_3 < y < b_4,\ 0 < z < c\}, \end{aligned} \tag{2}$$

in the copper

$$\begin{aligned} &\frac{\partial u}{\partial t} = D_3\Big(\frac{\partial^2 u}{\partial x^2} + \frac{\partial^2 u}{\partial y^2} + \frac{\partial^2 u}{\partial z^2}\Big), \\ &\Omega_1'' = \{0 < x < a,\ 0 < y < b_1,\ 0 < z < c\}, \\ &\Omega_2'' = \{0 < x < a,\ b_4 < y < b_5,\ 0 < z < c\}. \end{aligned} \tag{3}$$

The initial condition specifies temperature distribution in the medium at the origin of the time coordinate $t = 0$:

$$\begin{aligned} &u|_\Omega = u(0, x, y, z) = u_0, \\ &\Omega = \{0 \le x \le a,\ 0 \le y \le b_5,\ 0 \le z \le c\}, \end{aligned} \tag{4}$$

where u_0 – chosen temperature; Ω – whole investigated area.

The boundary conditions specify the temperature or the heat flow at the boundaries of the region:

$$\frac{\partial u}{\partial x}\Big|_{x=0;\, x=a} = 0, \quad \frac{\partial u}{\partial y}\Big|_{y=0;\, y=b_5} = 0, \quad \frac{\partial u}{\partial z}\Big|_{z=0;\, z=c} = 0, \tag{5}$$

$$
\begin{aligned}
D_2\frac{\partial u}{\partial y}\Big|_{y=b_1} &= D_3\frac{\partial u}{\partial y}\Big|_{y=b_1},\\
D_1\frac{\partial u}{\partial y}\Big|_{y=b_2} &= D_2\frac{\partial u}{\partial y}\Big|_{y=b_2},\\
D_2\frac{\partial u}{\partial y}\Big|_{y=b_3} &= D_1\frac{\partial u}{\partial y}\Big|_{y=b_3},\\
D_3\frac{\partial u}{\partial y}\Big|_{y=b_4} &= D_2\frac{\partial u}{\partial y}\Big|_{y=b_4},\\
u|_{\Psi} &= const,
\end{aligned}
\tag{5}
$$

here Ψ liquid channels in copper. The xy – plane cut boundary conditions are shown in Fig. 2.

We took pump profile to be Gaussian in x and y directions and also centered in these directions and in z direction $e^{-\gamma z}$. Thus the light source is described by a product of super-Gaussian functions:

$$
\begin{aligned}
f(x,y,z) = A\cdot\exp\Big(-2\big((x-a/2)/\alpha\big)^{10}\Big)\\
\cdot\exp\Big(-2\big((y-(b_3+b_2)/2)/\beta\big)^{2}\Big)\cdot\exp(-\gamma z),
\end{aligned}
\tag{6}
$$

where A is the integral power coefficient. This coefficient is obtained from the equality

$$
A=\frac{P^{\star}\cdot\big(1-\exp(-\gamma z)\big)}{\int\limits_{b_2}^{b_3}\int\limits_{0}^{a}\exp\Big(-2\big((x-a/2)/\alpha\big)^{10}\Big)\cdot\exp\Big(-2\big((y-(b_3+b_2)/2)/\beta\big)^{2}\Big)dxdy},
\tag{7}
$$

where $P^{\star} = P\cdot K$, P is the power, W; K the quantum defect, i.e., the coefficient which shows how much of the power transfers into heat.

The temperature in the crystal increases when the laser beam shoots to the crystal. Because of the increasing temperature, the crystal can be deformed or simply decomposed. In order to avoid this, we have to place over and under the laser crystal refrigerating slabs. Since the biggest temperature is in the middle of the crystal, i.e., at $x = a/2$, the cooling functions will also attain minimum values there. The liquid pipes in copper have to minimize temperature gradients. When the crystal is lightened by the lighting source, it is important that the temperature gradient $\max\limits_{[0,a]}\left|\frac{\partial u}{\partial x}\right|$ would not be too big. Thus, the minimization problem is to find $\min\max\limits_{[0,a]}\left|\frac{\partial u}{\partial x}\right|$.

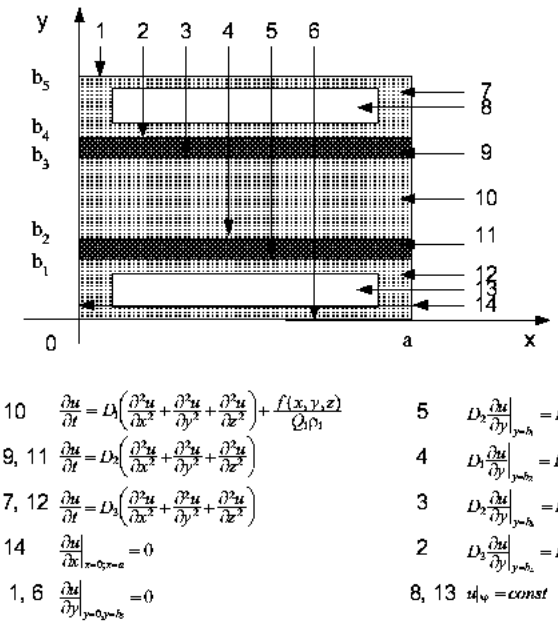

Fig. 2. The boundary conditions in the xy-plane cut.

3 Numerical Solution

Analytical solutions of most of the problems exist only in the simplest cases. Most science and engineering problems are comprised of complex geometrical and loading configurations making an analytical solution impossible. In order to obtain a solution, a numerical solution technique must be employed. We shal use the finite-difference technique. Let us introduce the following uniform grid:

$$x = x_0 + ih_1,\ i = 0, 1, \ldots, N_1,\ x_0 = 0,\ x_{N_1} = a,\ h_1 = \frac{a}{N_1},$$

$$y = y_0 + jh_2,\ j = 0, 1, \ldots, N_2,\ y_0 = 0,\ y_{N_2} = b_5,\ h_2 = \frac{b_5}{N_2},$$

$$z = z_0 + sh_3,\ s = 0, 1, \ldots, N_3,\ z_0 = 0,\ z_{N_3} = c,\ h_3 = \frac{c}{N_3},$$

$$t = n\tau,\ n = 0, 1, \ldots, M,\ \tau = \frac{T}{M}.$$

Set $u(t, x, y, z) = u\big(t(n), x(i), y(j), z(s)\big) = u(n, i, j, s) = u^n_{ijs}$.

We use an explicit scheme where our differential equations are replaced by the following difference equations:

$$u_{ijs}^{n+1} = g_1(u_{i+1,j,s}^n + u_{i-1,j,s}^n) + g_2(u_{i,j+1,s}^n + u_{i,j-1,s}^n) + g_3(u_{i,j,s+1}^n + u_{i,j,s-1}^n) + (1 - 2g_1 - 2g_2 - 2g_3)u_{ijs}^n + \frac{\tau f_{ijs}}{Q_1\rho_1}$$

for $1 \le i \le N_1 - 1,\ N_{22} + 1 \le j \le N_{23} - 1,\ 1 \le s \le N_3 - 1,$

$$u_{ijs}^{n+1} = g_1^*(u_{i+1,j,s}^n + u_{i-1,j,s}^n) + g_2^*(u_{i,j+1,s}^n + u_{i,j-1,s}^n) + g_3^*(u_{i,j,s+1}^n + u_{i,j,s-1}^n) + (1 - 2g_1^* - 2g_2^* - 2g_3^*)u_{ijs}^n$$

for $1 \le i \le N_1 - 1,\ N_{23} + 1 \le j \le N_{24} - 1,\ 1 \le s \le N_3 - 1,$

$$u_{ijs}^{n+1} = g_1^{**}(u_{i+1,j,s}^n + u_{i-1,j,s}^n) + g_2^{**}(u_{i,j+1,s}^n + u_{i,j-1,s}^n) + g_3^{**}(u_{i,j,s+1}^n + u_{i,j,s-1}^n) + (1 - 2g_1^{**} - 2g_2^{**} - 2g_3^{**})u_{ijs}^n$$

for $1 \le i \le N_1 - 1,\ N_{24} + 1 \le j \le N_2 - 1,\ 1 \le s \le N_3 - 1,$

$$g_k = \frac{\tau D_1}{h_k^2},\ g_k^* = \frac{\tau D_2}{h_k^2},\ g_k^{**} = \frac{\tau D_3}{h_k^2},\ k = 1, 2, 3.$$

The initial condition is approximated by

$$u_{ijs}^0 = u_0,\ 0 \le i \le N_1,\ 0 \le j \le N_2,\ 0 \le s \le N_3.$$

The boundary conditions are approximated by

$$u_{0,j,s}^n = u_{1,j,s}^n,\ u_{N_1,j,s}^n = u_{N_1-1,j,s}^n,$$
$$u_{i,N_{21},s}^n = (D_3 u_{i,N_{21}-1,s}^n + D_2 u_{i,N_{21}+1,s}^n)(D_3 + D_2),$$
$$u_{i,N_{22},s}^n = (D_2 u_{i,N_{22}-1,s}^n + D_1 u_{i,N_{22}+1,s}^n)(D_2 + D_1),$$
$$u_{i,N_{23},s}^n = (D_1 u_{i,N_{23}-1,s}^n + D_2 u_{i,N_{23}+1,s}^n)(D_1 + D_2),$$
$$u_{i,N_{24},s}^n = (D_2 u_{i,N_{24}-1,s}^n + D_3 u_{i,N_{24}+1,s}^n)(D_2 + D_3),$$
$$u_{i,N_{25},s}^n = u_{i,N_{25}-1,s}^n,$$
$$u_{i,j,0}^n = u_{i,j,1}^n,\ u_{i,j,N_3}^n = u_{i,j,N_3-1}^n$$

for $0 \le i \le N_1,\ 0 \le j \le N_2, 0 \le s \le N_3$, and $u_{ijs}^n = const,\ (i,j,s) \in \Psi$. The function $f(x,y,z)$ which stands for the lighting source is approximated by

$$f_{ijs} = A \cdot e^{-2\left(\frac{x_i - \frac{a}{2}}{\alpha}\right)^{10}} \cdot e^{-2\left(\frac{y_j - \frac{b_3 + b_2}{2}}{\beta}\right)^2} \cdot e^{-\gamma z_s}.$$

The integral power constant A is obtained from the relation:

$$A = \frac{1}{\int_0^a \int_{b_2}^{b_3} e^{-2\left(\frac{x_i - \frac{a}{2}}{\alpha}\right)^{10}} e^{-2\left(\frac{y_j - \frac{b_3+b_2}{2}}{\beta}\right)^{2}} dxdy} \cdot P^* \cdot (1 - e^{-\gamma c}).$$

We also examine a corresponding model in 2-D-in-space formulation of the model. The formulation can be rather easily derived from (1)–(5) by ignoring space coordinate z.

4 Results of Calculations and Discussion

The cooling system represented above is a good solution for a slab diode-pumped solid-state laser (most of the compact diode-pumped solid-state laser producers use a similar system). Moreover, this system is relatively compact. A large amount of cooling liquid is available. Water does not decompose and has the advantage of being optically stable under light expositions, it also has a high specific heat and thermal conductivity.

The numerical analysis was made with the values showed in Table 1. The necessary physical properties of the materials used are presented in Table 2.

Table 1. The values needed for calculations

Parameter	Value
Yb:KGW, sapphire, copper plates width, a	3 mm
Yb:KGW, sapphire, copper plates length, c	3 mm
Yb:KGW plate height b',	0.5 mm
Copper plate height, b''	1 mm
Sapphire plate height, b'''	0.35 mm
Spot parameters: α, β, γ	0.8 mm, 0.1 mm, 1.7 mm
Pump power, P	2.4 W
Quantum defect, K	7 %
Liquid temperature, u^*	0–15 °C

Water is chosen as a liquid for the cooling system. Water channel is 0.25 mm high × 1.5 mm wide.

The 3-D and 2-D-in-space models were compared with one another in place where pump beam enter the laser crystal. In both cases the maximum

Table 2. Physical properties of laser materials used for modelling

Sub domain	Material	Q – specific heat $[\mathrm{J/g \cdot K}]$	k – thermal conductivity $[\mathrm{W/mm \cdot K}]$	ρ – density $[\mathrm{g/mm^3}]$
1	Yb:KGW	0.5	0.003	0.00717
2	sapphire	0.784	0.0351	0.00398
3	copper	0.395	0.39	0.00893

temperature was achieved at the entrance of the pumping area. As Fig. 3 shows, there is no difference between the 2-D and 3-D models when calculating the steady-state temperature at any point of the system.

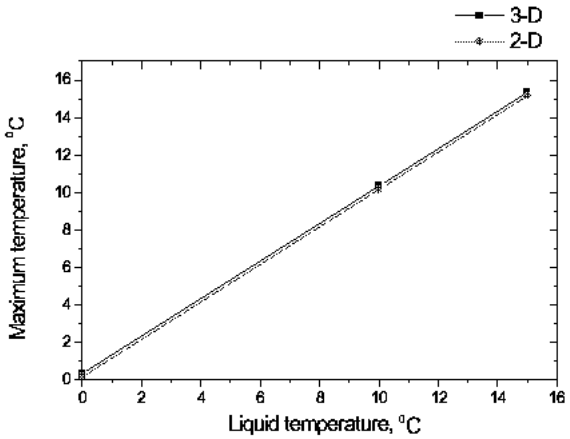

Fig. 3. The achieved maximum temperature dependence on liquid temperature in both cases: two dimensional and three dimensional model in space.

From the results of computation it follows that temperature dependence on time is the same for both 2-D and 3-D models. The results of these calculations are shown in Fig. 4.

Figure 5 and Fig. 6 show the results of calculated steady-state temperature in yz-plane cut and the temperature profile for 2.4 W pump power with the bottom and top cooling. In these figures, the results of the calculation for the 3-D model are shown (Fig. 6 is for the 2-D model).

From the above-dicussed results one conclusion can be done. The reliability of two-dimensional model for the temperature calculation is very good.

There is no reason for using the 3-D model, because the 2-D model is good enough. It contains less parameters, it takes less computational time and the steady-state temperature calculated in both cases is the same.

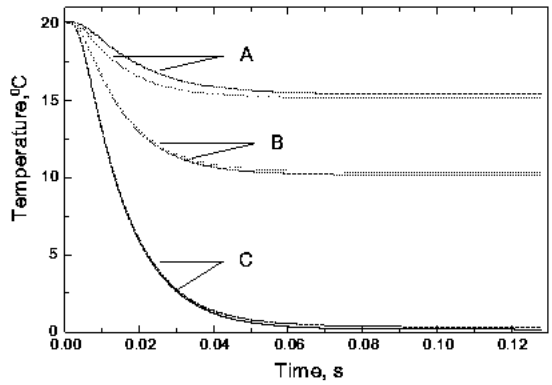

Fig. 4. The temperature dependence on time. A: 2-D and 3-D models, the liquid temperature is 15°C; B: 2-D and 3-D models, the liquid temperature is 10°C; C: 2-D and 3-D models, the liquid temperature is 0°C; in A, B and C cases the upper curves is for 2-D model, lower – for 3-D model.

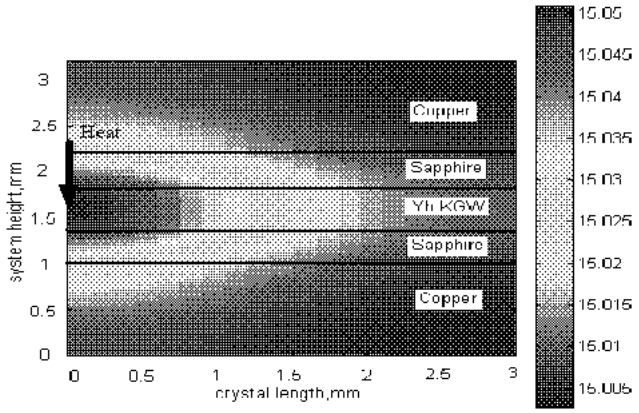

Fig. 5. The results of calculated temperature field in yz-plane cut in the system. The system contains Yb:KGW laser crystal, 2 sapphire slabs and 2 copper slabs with water channels in it.

The following calculations were made to find the temperature gradient in

the laser material. The biggest temperature is in the middle of the crystal, it is important that the temperature gradient $\max_{[0,a]} \left|\frac{\partial u}{\partial x}\right|$ at $x = a/2$ would not be too big. We compared 2-D and 3-D models for the temperature gradient and found that they differ 2 times. The resuls are shown in Table 3.

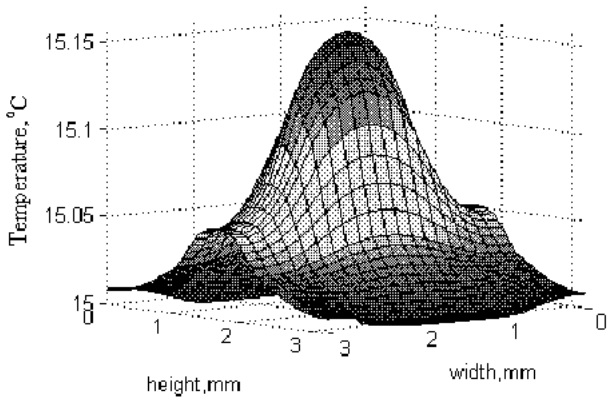

Fig. 6. Temperature profile for 2.4 W pump power with the bottom and top cooling. The cooling liquid temperature is 15°C.

Table 3. The calculated temperature gradients

Model	Liquid temperature [°C]	Temperature gradient [°C/mm]	Time [s]
2-D	10	0.288	1.8
2-D	15	0.288	1.8
3-D	10	0.177	1.8
3-D	15	0.177	1.8

Another important task was to find the conditions when the temperature gradient is small. This problem can be solved by choosing the water channel more comparable to a spot size. If the spot width is $2\alpha = 0.2$ mm (0.6 mm and 1.5 mm, respectively), the temperature gradient is 1.33°C/mm (0.7°C/mm and 0.2°C/mm, respectively). The temperature dependence on spot width for the 2-D model is shown in Fig. 7.

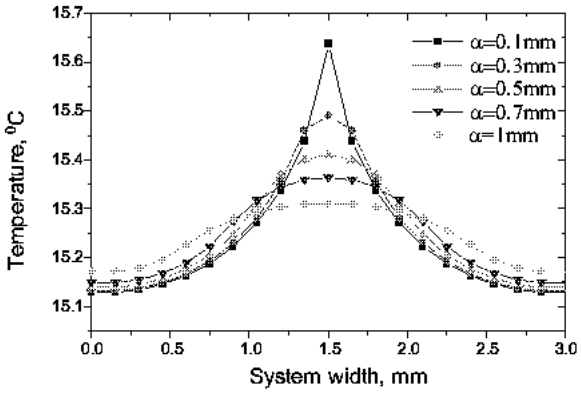

Fig. 7. The temperature dependence on spot width: $\alpha = 0.1$ mm – temperature gradient is 1.33 °C/mm; $\alpha = 0.3$ mm – temperature gradient is 0.701 °C/mm; $\alpha = 0.5$ mm – temperature gradient is 0.424 °C/mm; $\alpha = 0.7$ mm – temperature gradient is 0.343 °C/mm; $\alpha = 1$ mm – temperature gradient is 0.22 °C/mm.

5 Conclusions

1. Comparing two dimensional and three dimensional in space models during the same time the achieved temperature is the same.

2. The temperature gradient in the 2-D model is two time higher than in 3-D model. If our aim is to calculate the temperature gradient in the x direction, the three-dimensional model is preferable.

3. In order to get the lower temperature gradient, the width of the liquid channel must be comparable with the spot width in both the 2-D and 3-D models.

References

1. Fan T. Y. "Heat generation Nd:YAG", *IEEE J. of Quantum Electronics*, **29**, p. 1457–1459, 1993

2. Paschotta R., Aus der Au J., Keller U. "Thermal effects in high-powered-pumped lasers with elliptical-mode geometry", *IEEE J. of Quantum electronics*, **6**(4), p. 636–642, 2000

3. Koechner W. *Solid State Laser Engineering*, 4th ed. Spring-Verlag, Berlin, p. 396, 1996

4. http://www.geocities.com/EnchantedForest/Creek/9660/PPSSL.htm

5. Samarskii A.A. *The Theory of Difference Schemes,* Nauka, Moscow, 1989 (in Russian)

6. Baronas R., Ivanauskas F., Sapagovas M. "Reliability of one dimensional model of moisture diffusion in wood", *Informatica,* **13**(4), p. 405–416, 2002